ARL-MR-0908 ● SEP 2015

US Army Research Laboratory

Microscale Alloy Type Lithium Ion Battery Anodes

by Collin R Becker

NOTICES

Disclaimers

The findings in this report are not to be construed as an official Department of the Army position unless so designated by other authorized documents.

Citation of manufacturer's or trade names does not constitute an official endorsement or approval of the use thereof.

Destroy this report when it is no longer needed. Do not return it to the originator.

ARL-MR-0908 ● SEP 2015

US Army Research Laboratory

Microscale Alloy Type Lithium Ion Battery Anodes

by Collin R Becker
Sensors and Electron Devices Directorate, ARL

REPORT DOCUMENTATION PAGE

Form Approved
OMB No. 0704-0188

1. REPORT DATE *(DD-MM-YYYY)*	2. REPORT TYPE	3. DATES COVERED (From - To)
September 2015	Final	

4. TITLE AND SUBTITLE
Microscale Alloy Type Lithium Ion Battery Anodes

5a. CONTRACT NUMBER

5b. GRANT NUMBER

5c. PROGRAM ELEMENT NUMBER

6. AUTHOR(S)
Collin R Becker

5d. PROJECT NUMBER

5e. TASK NUMBER

5f. WORK UNIT NUMBER

7. PERFORMING ORGANIZATION NAME(S) AND ADDRESS(ES)
US Army Research Laboratory
ATTN: RDRL-SED-C
2800 Powder Mill Road
Adelphi, MD 20783-1138

8. PERFORMING ORGANIZATION REPORT NUMBER
ARL-MR-0908

9. SPONSORING/MONITORING AGENCY NAME(S) AND ADDRESS(ES)

10. SPONSOR/MONITOR'S ACRONYM(S)

11. SPONSOR/MONITOR'S REPORT NUMBER(S)

12. DISTRIBUTION/AVAILABILITY STATEMENT
Approved for public release; distribution unlimited.

13. SUPPLEMENTARY NOTES

14. ABSTRACT
The fabrication of microscale anodes designed for in situ atomic force microscopy testing is discussed. The anodes are partially confined in a nickel thin film and contain enough active material to be successfully used with conventional electrochemical testing methods. The electrodes are characterized by Raman spectroscopy, scanning electron microscopy, and atomic force microscopy.

15. SUBJECT TERMS
battery lithium silicon microfabrication

16. SECURITY CLASSIFICATION OF:			17. LIMITATION OF ABSTRACT	18. NUMBER OF PAGES	19a. NAME OF RESPONSIBLE PERSON
a. REPORT	b. ABSTRACT	c. THIS PAGE			Collin R Becker
Unclassified	Unclassified	Unclassified	UU	16	19b. TELEPHONE NUMBER (Include area code) 301-394-0476

Contents

List of Figures

1. Introduction

Alloy-type anodes show tremendous promise to enhance the capacity of lithium (Li) ion batteries.[1–3] Silicon (Si), germanium (Ge), tin (Sn), and aluminum (Al) all can alloy with Li at low electrochemical potentials relative to Li/Li+.[4,5] At the high end, Si can store more than 10 times the amount of Li than the state-of-the-art anode material, graphite, can store.[1] Unfortunately, these materials also undergo an approximately 300% volume expansion during the alloy process.[6] As the materials are cycled, cracks begin to form, and the material fractures and breaks apart. This fracture process also leads to an unstable solid electrolyte interphase (SEI) and further capacity loss.

An extraordinary amount of work has been done in an effort to solve this fundamental problem with the material. While reducing the size of the material to the nanoscale or implementing as a thin film helps to mitigate the failure of the material, it has not solved the problem. Researchers have taken several approaches to studying the material, including making powders of varying composition, growing thin films, in situ transmission electron microscopy (TEM) testing of single particles, computational simulation, and in situ atomic force microscopy (AFM) testing.[1,5,7–9] The in situ AFM testing confers the benefits of visualizing nano- and microscale particles in conventional electrolytes with the ability to use conventional electrochemical testing.

This report discusses the fabrication procedure for a new type of in situ AFM battery test bed for these alloy materials. Along with the microfabrication procedure, results from Raman spectroscopy and scanning electron microscopy (SEM) and AFM are presented. Additionally, the fabrication of a smooth nickel (Ni) current collector that is critical to the success of the AFM imaging is discussed.

2. Experimental

As in a prior tech report, having a smooth surface is critical for AFM analysis.[10] Here we make use of an ion source in an Evatek BAK 641 electron beam evaporator. The ion source is a Veeco Mark II Controller that is operated at a voltage between 160–300 V, an amperage between 2–6 A (the max power for the controller) and a mean pressure in the chamber during deposition of ~2.1×10^{-4} mbar. The Veeco controller has unknown errors often when running at full power, so the lower power recipes were also evaluated. As seen in Fig. 1, while the lower power recipes produce adequately smooth films, the higher power settings clearly have smoother surfaces. The total thickness of the Ni layer is 400 nm and the deposition rate is set at 0.2 nm/s.

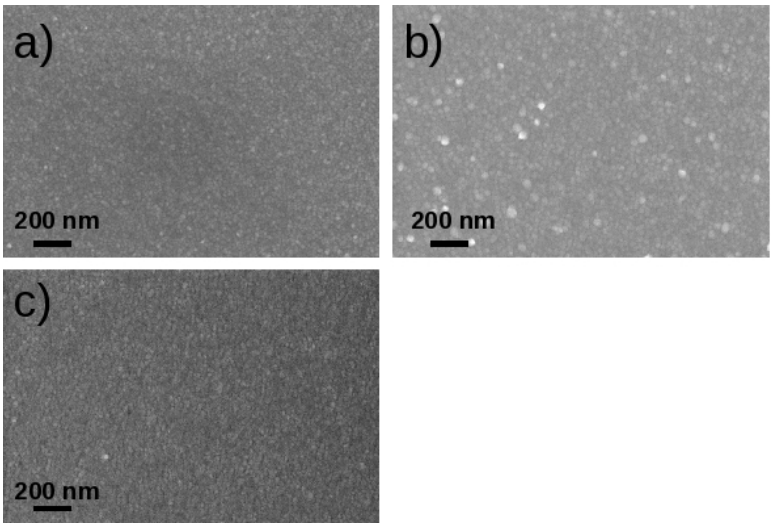

Fig. 1 SEM images of the Ni films with the ion source operating at a voltage and amperage of a) 180 V and 4 A, b) 160 V and 2 A, and c) 300 V and 6 A

It is noted that with the ion source and because of the increased gas pressure and lack of directionality of ions, metal will be deposited partially on the backside of the wafer. If this is an issue, the backside might be protected with a layer of photoresist or hard mask that could be etched at a later time.

As shown in Fig. 2, for the fabrication flow of the samples, the next step is to deposit and pattern photoresist on the wafer. The photoresist development consists of coating the wafer with a layer of vapor hexamethyldisilazane (HMDS) at 140 °C, spinning 5214 reverse image photoresist at 2000 rpm for 45 s, and then performing a prebake at 110 °C for 75 s. Next the wafer is exposed to ultraviolet (UV) light through a chrome mask under vacuum contact in a Karl Suss MA6 aligner for 5 s at 9.4 mW/cm^2 total power (8.0 mW/cm^2 at 365 nm and 20.2 mW/cm^2 at 405 nm). The wafer is then postbaked at 120 °C for 40 s on a vacuum hotplate. This is the most critical step of the process and a quality hotplate with reproducible temperature should be used. Next a 10-s flood UV exposure is used. Finally, the wafer is developed for 55–60 s in 400 K 1:4 diluted developer. All coat and bake steps are carried out in an EVG 120 system and the development is done by hand in a bath of approximately 150 ml of developer. Prior to ion milling, a UV hard bake cure is performed in an Axcelis Fusion 200. The chrome mask pattern is 5 μm diameter circles spaced by 10 μm center to center.

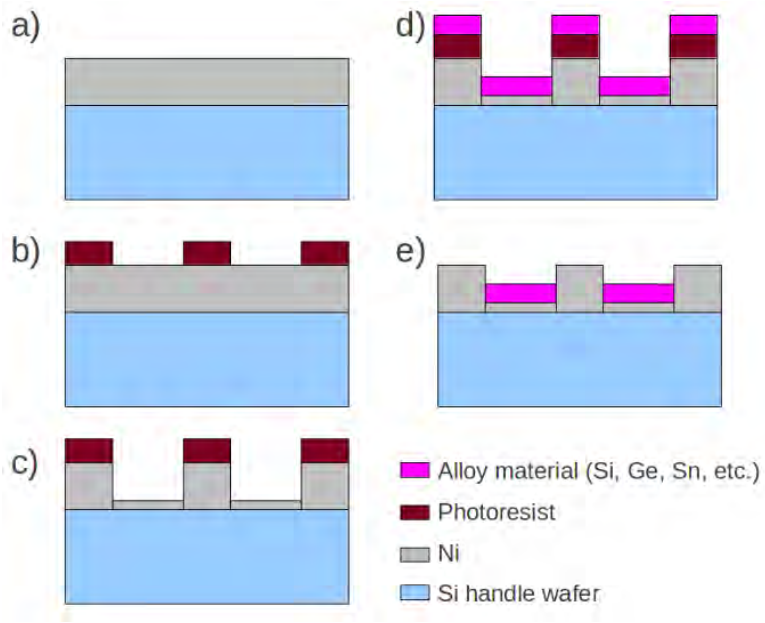

Fig. 2 Fabrication flow of electrode test bed structures. a) A Ni film is evaporated on the Si handle wafer. b) Photoresist is coated and patterned on the Ni film. c) The Ni film is ion milled. d) Ni is deposited into the holes created by the ion milling. e) Liftoff is performed to remove the photoresist and Ni film on top of the photoresist.

Following photoresist patterning, the wafers are ion milled. The ion milling tool is manufactured by 4wave Instruments. The milling is accomplished in 2 etch steps, 1 at 95° and 1 at 140°. The milling time is 370 s at 90° and 50 s at 140°. The etch time was chosen to mill at least 200 nm into the substrate but not cross into the Si handle wafer.

After ion milling, a 20-nm Ni adhesion layer, and a 100-nm Si layer are deposited into the pits now in the Ni film using the Evatek evaporator. The deposition rate is 0.2 nm/s and the pressure is ~2×10^{-6} mbar. No ion-assist source is used in this step. Lastly, the wafers are immersed in the n-methyl-2-pyrolidone (NMP) based PRS-3000 (JT Baker) photoresist remover at 80 °C for several hours and then rinsed in water.

3. Discussion and Results

Figure 3 presents the results from a Raman spectroscopy study of the samples. A Renishaw Invia microscope with a 2400-l/mm grating and a 532-nm laser is used to determine the crystallinity of the Si pits. The mapping function of the microscope clearly reveals that the Si pits are amorphous Si and no Si is present between the pits. Thus the pits will behave as separate regions of material when tested and Li ion battery anode. Additionally, the pits create a confined region to compress the Si as it expands during lithiation.

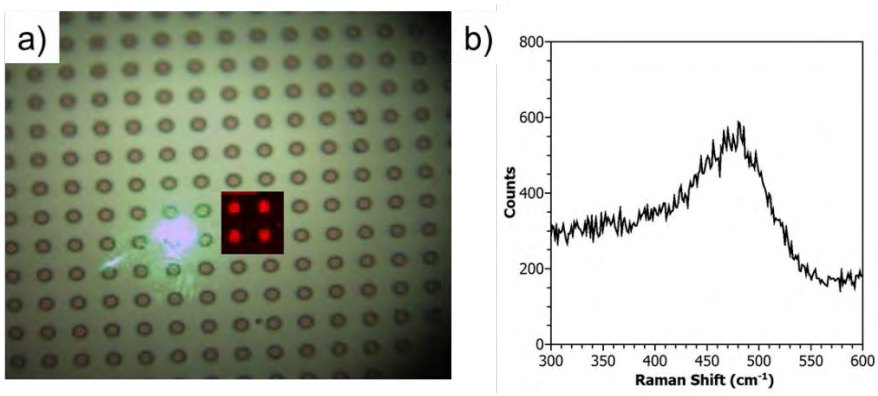

Fig. 3 a) A Raman map of the battery test beds where the inset shows regions corresponding to the representative Raman spectra in b), which reveals an amorphous Si peak

An AFM region in Fig. 4 shows the surface topography of the chip. The very smooth Ni film, with a root mean square (RMS) roughness of 1.3 nm is an excellent reference to measure changes in height of the Si material when it expands and contracts during Li ion battery testing. The pit is about 225 nm deep. Since 100 nm of Si and 20 nm of Ni were deposited into the ion milled pits, this indicated the ion milling was 350 nm deep. The ion milling time was 370 s, which equates to an etch rate of 0.95 nm/s, or 0.83 nm/s if the 50 s of high angle milling are included.

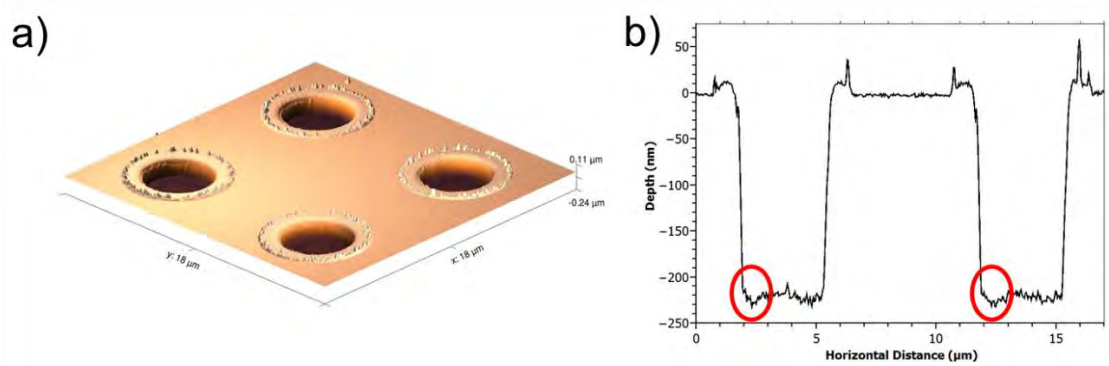

Fig. 4 An AFM image a) and line profile b) of the pits after being filled with evaporated Si. The red circles highlight a small dip in the pits near the Ni wall.

A ridge of material is also seen at the top of the pit. The height of this ridge is on the average ~20 nm tall, with some spikes that are closer to 50 nm tall. Since 120 nm of Ni and Si were deposited into the pits, it is unlikely that this ridge is composed of the evaporated Si and Ni. It is more likely that this is the result of redeposition of Ni during the ion milling process. The negative profile of the 5214 photoresist would provide a pocket where the Ni atoms could collect as they are milled from the thin film. This process may occur during the initial milling when the pit is shallow and while most Ni atoms will leave the pit in the vertical direction,

some may collect in the negative resist pocket. The deposition could be hardened photoresist as well as the wafer can be heated during the ion mill process. Electrochemical testing may provide insight in the composition of the ridge. If the ridge expands and contracts, then it is composed of Si that alloys with Li, otherwise the ridge is most likely redeposited Ni.

The SEM image in Fig. 5 shows an SEM cross section of the pits. Based on the image contrast of the materials, the Ni film, the 20-nm Ni adhesion layer, and the 100-nm Si layer can readily be observed. Interestingly, it appears that Si does not wet the Ni wall and there is some free space. This shows in the profile taken by the AFM as well with the red circles in Fig. 4 highlighting the small dip in the profile.

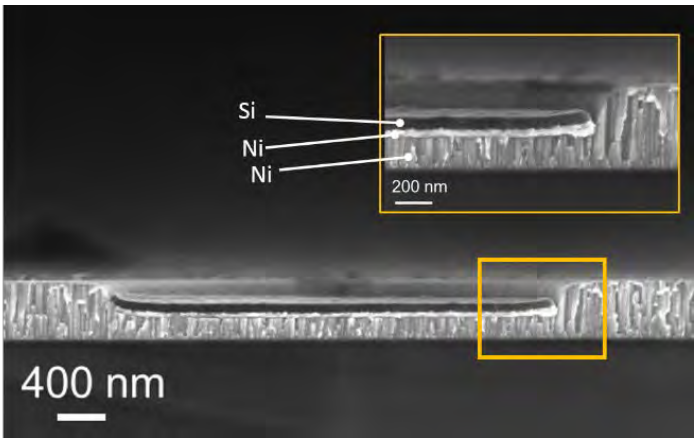

Fig. 5 SEM cross section of the pits showing the Ni layer and thin film Si

From the SEM image in Fig. 6a, the actual fabricated diameter of the pits is about 3.9 µm. Assuming a density of 2.33 g/cm^3 and an energy capacity of Si of 4200 mAh/g, the total capacity of each chip that will be tested is 19.8 µAh. This is enough active material that the capacity of a chip can be tested even in an electrochemical cell that is flooded with electrolyte and will have some amount of parasitic reactions.

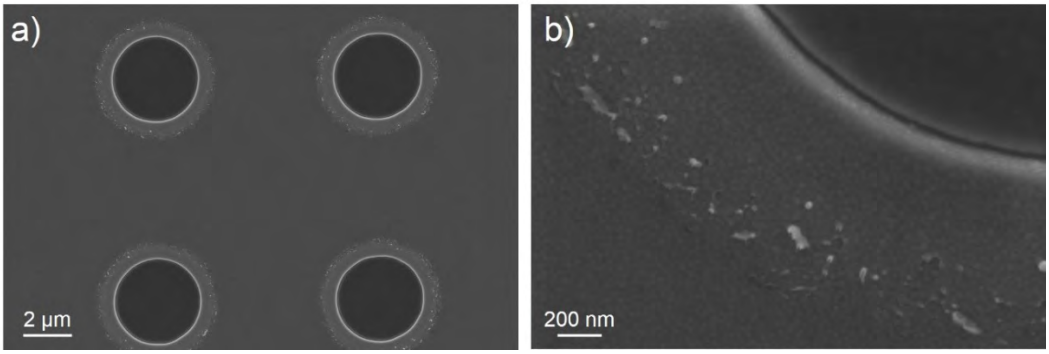

Fig. 6 SEM images of the Si pits a) and a high magnification image of the redeposited material near the edge of the pit b)

4. Conclusion

Alloy-based electrodes have been microfabricated so that they are partially confined in a metal current collector. The current collector has been optimized by ion assisted electron beam evaporation to be very smooth to enable future AFM investigations to have as flat as baseline as possible. This template should allow interesting in situ Li ion battery studies to occur.

5. References

1. Becker CR, Strawhecker KE, McAllister QP, Lundgren CA. ACS Nano. 2013;7(10):9173–9182.
2. Chan CK, Zhang XF, Cui Y. Nano Lett. 2008;8(1):307–309.
3. Chan CK, Peng H, Liu G, McIlwrath K, Zhang XF, Huggins RA, Cui Y. Nat. Nanotechnol. 2008;3(1):31–35.
4. Beaulieu LY, Eberman KW, Turner RL, Krause LJ, Dahn JR. Electrochem. Solid State Lett. 2001;4(9):A137–A140.
5. Duveau D, Fraisse B, Cunin F, Monconduit, L. Chem. Mater. 2015;27(9):3226–3233.
6. McAllister QP, Strawhecker KE, Becker CR, Lundgren CA. J. Power Sources. 2014.
7. Liu XH, Liu Y, Kushima A, Zhang S, Zhu T, Li J, Huang JY. Adv. Energy Mater. 2012;2(7):722–741.
8. Abel PR, Lin Y-M, Celi, H, Heller A, Mullins CB. ACS Nano. 2012;6(3):2506–2516.
9. Lee SW, McDowell MT, Choi J, W, Cui Y. Nano Lett. 2011;11(7):3034–3039.
10. Becker CR, Strawhecker KE, Ligda JP, Lundgren CA. Microfabricated Amorphous Silicon Nanopillars on an Ultrasmooth 500-nm-thick Titanium Adhesion Layer. Adelphi (MD): Army Research Laboratory (US); 2012 Sep. Report No.: ARL-TR-6209.

List of Symbols, Abbreviations, and Acronyms

AFM	atomic force microscopy
Al	aluminum
Ge	germanium
HMDS	hexamethyldisilazane
Li	lithium
Ni	nickel
NMP	n-methyl-2-pyrolidone
RMS	root mean square
SEI	solid electrolyte interphase
SEM	scanning electron microscopy
Si	silicon
Sn	tin
TEM	transmission electron microscopy
UV	ultraviolet

1 (PDF)	DEFENSE TECH INFO CTR DTIC OCA
2 (PDF)	US ARMY RSRCH LAB IMAL HRA MAIL & RECORDS MGMT RDRL CIO LL TECHL LIB
1 (PDF)	GOVT PRNTG OFC A MALHOTRA
1 (PDF)	US ARMY RSRCH LAB RDRL SED C C BECKER

INTENTIONLLY LEFT BLANK.